Journal of the Peripheral Nervous System 10:369–374 (2005)

RESEARCH REPORT

Ultrasound imaging of the rabbit peroneal nerve

B. S. de Kool[1,2], Johan W. van Neck[1], Joleen H. Blok[2], Erik T. Walbeehm[1], Ineke Hekking[1], and Gerhard H. Visser[2]

[1]*Department of Plastic and Reconstructive Surgery; and* [2]*Department of Clinical Neurophysiology, Erasmus MC, Rotterdam, the Netherlands*

Abstract Ultrasound imaging of peripheral nerves is increasingly used in the clinic for a wide range of applications. Although yet unapplied for experimental neuroscience, it also has potential value in this research area. This study explores the feasibility, possibilities and limitations of this technique in rabbits, with special focus on peripheral nerve regeneration after trauma. The peroneal nerve of 25 New Zealand White rabbits was imaged at varying time intervals after a crush lesion. The ultrasonic appearance of the nerve was determined, and recordings were validated with *in vivo* anatomy. Nerve swelling at the lesion site was estimated from ultrasound images and compared with anatomical parameters. The peroneal nerve could reliably be identified in all animals, and its course and anatomical variations agreed perfectly with anatomy. Nerve diameters from ultrasound were related to *in vivo* diameters ($p < 0.001$, $R^2 = 77\%$), although the prediction interval was rather wide. Nerve thickenings could be visualized and preliminary results indicate that ultrasound can differentiate between neuroma formation and external nerve thickening. The value of the technique for experimental neuroscience is discussed. We conclude that ultrasound imaging of the rabbit peroneal nerve is feasible and that it is a promising tool for different research areas within the field of experimental neuroscience.

Key words: nerve imaging, peroneal nerve, rabbits, regeneration, ultrasonography

Introduction

Since the introduction of high-frequency linear array transducers in the mid 90s, ultrasound imaging of peripheral nerves is widely gaining application as a diagnostic tool. Indications include diagnosis of nerve compressions *(Beekman and Visser, 2003)*, nerve lesions *(Peer et al., 2003)*, perineural fibrosis *(Quinn et al., 2000)*, nerve tumours *(Stuart et al., 2004)*, and hereditary neuropathies *(Beekman and Visser, 2002)*. In carpal tunnel syndrome, nerve diameters have been proven to relate to electromyography *(Lee et al., 1999)*.

Address correspondence to: B. S. de Kool, Department of Clinical Neurophysiology, D-Ba 451, Erasmus MC, PO Box 2040, 3000 CA, Rotterdam, the Netherlands. Tel: +31-10-463-3765; Fax: +31-10-463-4621; E-mail: koolifix@yahoo.ie

Although often applied clinically, no studies have been published on ultrasound imaging of the much smaller nerves of the rabbit, although this animal is frequently used as an experimental model in neuroscience. This technique could be very useful in, for example, studies on nerve regeneration, nerve thickening neuropathies and tumour formation. In nerve regeneration studies, ultrasound imaging has a potential value for determining the quality of the lesion site (neuroma formation) and quantifying regeneration.

This study was designed to evaluate the feasibility of ultrasound imaging of the rabbit peroneal nerve and to explore its possibilities and limitations for experimental neuroscience, with special focus on regeneration after nerve trauma. We determined the ultrasonic appearance of the nerve and compared its course, its diameter and the presence of anatomical variations

Blackwell Publishing

and of nerve enlargement at the lesion site with *in vivo* anatomy.

Materials and Methods

Animals

For this study, 25 male New Zealand White rabbits weighing 3.0–5.6 kg were used. The experimental protocol was approved by the Animal Experiments Committee according to the National Experiments on Animals Act and conducted according to this law that serves the implementation of Directive 86/609/EC of the Council of Europe.

Surgery

Surgery and measurements were performed under general anaesthesia (1–2% isofluorane in a mixture of O_2/N_2O), preceded by Hypnorm injection (0.23 mL/kg, IM [intramuscular]). The right peroneal nerve was lesioned 1 cm distal to the trochanter major of the femur by crushing the nerve for 30 s with a 2-mm-wide surgical needle holder. Such a lesion destroys axonal continuity while leaving the epineurium intact. Animals received Baytril (10 mg/kg) from 1 day before to 2 days after surgery and Temgesic (0.03 mg/kg) for 2 days after surgery. Nerves were left to regenerate for varying periods ranging from 4 to 13 weeks. After this period, ultrasound imaging was performed on the lesioned nerve. After performing the measurements, animals were sacrificed through intravenous injection of an overdose of pentobarbital.

Ultrasound imaging

The right hind leg was shaved. The animal was positioned on its left side with both knees at a 90° angle and the feet in a natural position. In this position, the skin between the trochanter major and the knee lay quite flat, simplifying nerve scanning. The legs were taped to the operating table at the distal crease to keep the legs in position. The location of the trochanter major was marked on the skin as a reference for distance measurements. The skin was then wetted with 70% alcohol because this improved acoustic coupling, and a generous amount of ultrasound gel was applied.

Ultrasound imaging was performed on an Aloka SSD-3500 system with a UST-5542 High Frequency Linear Array probe (Aloka Co.). Settings used for nerve visualisation are given in Table 1. These settings were used as a fixed preset for all recordings. A beam frequency of 13 MHz was used to enable good resolution of the nerve interior. Acoustic power was kept low to avoid masking of the fine image details through saturation of the ultrasound intensity. The receiver gain was set at 60 dB because a higher gain blurred the image details.

The common peroneal nerve was imaged by scanning in transversal and longitudinal directions from the trochanter major to where the cranial portion of lateral head of the gastrocnemius muscle is perforated. Proximally, the peroneal and the tibial nerves lay next to each other, enclosed by an epineural sheet. To avoid confusing these nerves on longitudinal scanning, we first checked the course of the larger tibial nerve and then directed the ultrasound beam more anteriorly to find the peroneal nerve. To differentiate between nerves and two adjacent muscle fascias, the probe was moved back and forth in lateral direction while scanning longitudinally. Because the nerve is small and elliptical in form, lateral probe movement should result in decay of the observed diameter, which is not the case with the distance between two adjacent muscle fascias.

From transversal recordings, the diameter of the inner nerve border was measured at four locations: (1) at the trochanter major, (2) where the nerve first touched the gastrocnemius muscle, (3) where it perforated the lateral head of this muscle and (4) 1 cm proximal to site 3. In transversal images, we only measured the inner nerve diameter because the outer nerve border was less well defined in the transversal images. This is partly because an area of high or mixed echogenicity was often present around the nerve.

Appearance of the lesion was assessed from longitudinal recordings. Here, we measured both inner and outer nerve diameters at the lesion site because the outer nerve border is more easily delineated on longitudinal images. Similar longitudinal measurements at 4 cm distal to the trochanter major served as a reference to define local nerve thickening. Accuracy of the on-screen measurement tool was 0.1 mm.

Anatomical measurements

The peroneal nerve was dissected free along its entire length. *In vivo* nerve diameters were measured at the same sites of the ultrasound measurements. Diameters were measured with a calliper gauge (accuracy 0.1 mm) underneath a dissection microscope, before and after removing extraneural fat. The presence or absence of anatomical variations or abnormalities was assessed visually.

Analysis and statistics

A confidence level of 95% was used throughout the study. We estimated the predictive value of ultrasound diameters with regard to anatomical diameters through linear regression analysis after taking the natural logarithm of both diameters to obtain near-normal

Table 1. Machine settings used for nerve imaging.

	Value used	Available range
Frequency (MHz)	13	7–13
Gain (dB)	60	30–90
Acoustic power (%)	19	0–100
Contrast	4	0–15
Relief	0	0–3
Ac. gain compensation	2	0–15
Scan depth (cm)	2	2–24
Line density	3	1–3
Smoothing	4	1–8
Horizontal smoothing	1	0–2
Frame correlation	5	0–15

Right column shows the range of values available on our equipment. Ac., acoustic.

distributions. From this, the 95% prediction interval and the percentage variability explained by the relation (Pearson R^2) were calculated. Local thickening at the lesion site was defined as an increase of more than 0.5 mm in nerve diameter compared with that at 4 cm distal to the trochanter major, for both ultrasound and anatomy. After applying this cut-off, the positive and negative predictive values (PPV and NPV) of the ultrasound estimates were calculated for inner and outer diameters.

Results

Ultrasonic appearance

The peroneal nerve was found in all animals. Scanning and measuring the entire nerve in both longitudinal and transversal directions was accomplished in 70 min on average. Retrospective analysis of the images showed that, only on longitudinal scanning, in one case, the proximal part of the nerve was confused with the tibial nerve. Figures 1 and 2 show the ultrasonic appearance of the peroneal nerve in longitudinal and transversal aspects. The nerve consisted of a hypoechoic interior, surrounded by a hyperechoic rim. Often, an area of mixed or high echogenicity was found surrounding the nerve. Proximally, the nerve lay at its maximal depth and then moved superficially because it coursed distally. In this area, the larger tibial nerve could clearly be seen lying posterior to the peroneal nerve before they separated. The peroneal nerve then crossed a branch of the popliteal artery and emerged across the gastrocnemius muscle. Distally, it lay very superficial and clearly flattened. It then perforated the muscle and submerged again (Fig. 1). More distally, the nerve could not be followed reliably.

Because of its superficial course and characteristic flattened form distally, the nerve was best found at about 1–2 cm proximal to the knee. It could then be followed over its entire length in most animals up to about 0–1 cm distal to the trochanter major. Transversally, the nerve was sometimes difficult to image at the lesion site. In addition, around the trochanter major and at about 5–6 cm distal to this joint, the nerve borders were often less clear. Furthermore, a few animals had local skin areas of intensive hair growth, which were very echodense, resulting in acoustic shadowing. The latter problem could often be overcome by pulling the skin sideways, so that the region of interest became shadow free.

Ultrasound vs. anatomy

The concordance between ultrasonic and anatomical observations of nerve morphology was good. In all cases where the nerve course appeared normal on ultrasound, it was also normal anatomically. In two animals, the course of the peroneal nerve was abnormal. It crossed the tibial nerve and remained posterior to this nerve for some distance. In both the cases, this was clearly detected with ultrasound. Intraneural fascicles could normally not be seen. However, in one animal in which the peroneal nerve consisted of two separate branches and in another in which the tibial nerve had two clearly separate fascicles, these were well detectable on transversal scanning. In all other animals, transversal ultrasound did not reveal separate bundles, and they were also not seen upon anatomical exploration. On longitudinal scanning, however, there was one animal in which there seemed to be a separate bundle that was not present anatomically.

Figure 3 shows the relation between nerve diameters from ultrasound and those measured anatomically, together with the 95% prediction interval.

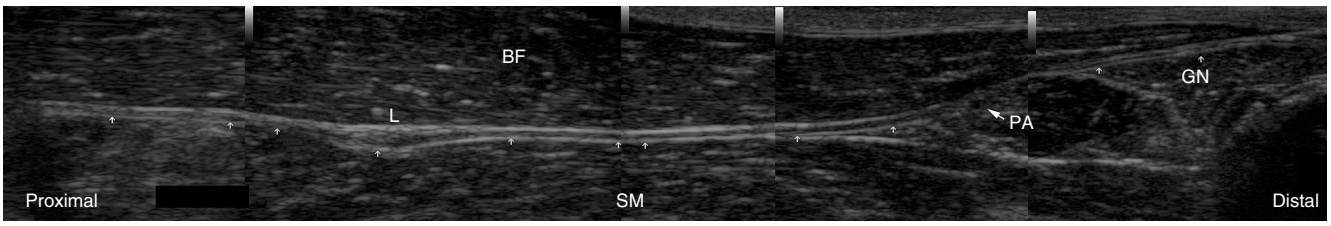

Figure 1. Ultrasonic appearance of the peroneal nerve in longitudinal aspect (L, lesion site; BF, biceps femoris muscle; SM, semimembranosus muscle; GN, gastrocnemius muscle; PA, branch of popliteal artery).

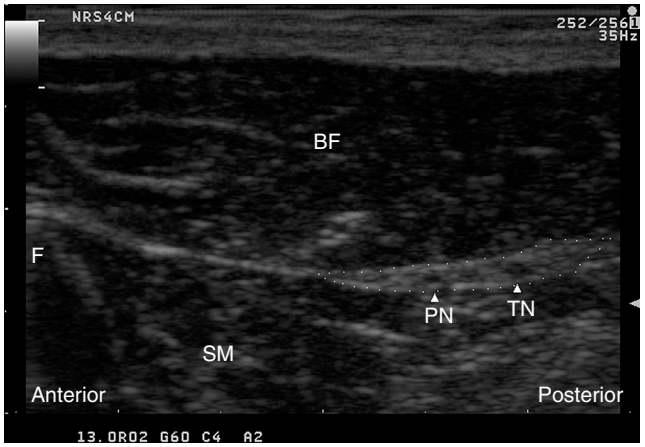

Figure 2. Ultrasonic appearance of the peroneal and tibial nerve in transversal aspect at 4 cm distal to the trochanter major of the femur. In this animal, the tibial and peroneal nerves have just split at this site (PN, peroneal nerve; TN, tibial nerve; BF, biceps femoris muscle; SM, semimembranosus muscle; F, femur). Dotted line – area of increased echogenicity, which was often found surrounding the nerves.

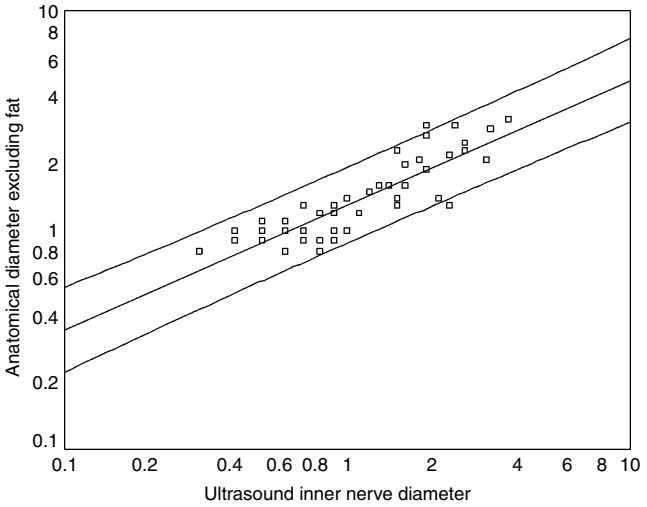

Figure 3. Relation between nerve diameters from ultrasound and those measured anatomically with 95% prediction interval. Data are ln-transformed to obtain near-normal sample distributions. $n = 56$.

The regression equation was estimated as $\ln(d_A) = 0.57 \ln(d_{US}) + 0.11$ mm (slope: $p < 0.001$, paired sample *t*-test, $n = 56$), in which d_A is the anatomical diameter (excluding fat) and d_{US} the diameter from ultrasound (inner nerve diameter). The percentage explained variability (R^2) was 77%.

Nerve thickening

Nerve thickening could be well visualised. In most animals, the hypoechoic nerve interior was clearly enlarged (Fig. 4), while in others, only the nerve border appeared thickened (Fig. 5). The predictive values from ultrasound regarding nerve swelling are summarized in Table 2. The one animal, in which the proximal part of the nerve was confused with the tibial nerve on longitudinal images, was excluded from this analysis.

Discussion

Ultrasonic appearance

This study shows that the rabbit peroneal nerve can be imaged well with ultrasound. In agreement with human studies, the nerve appeared as a hypoechoic structure with a hyperechoic border, both on transversal and longitudinal images *(Silvestri et al., 1995; Beekman and Visser, 2003)*. In human nerves, generally, multiple fascicles can be seen. Equivalently, in our study, the peroneal and tibial nerves, which together form the sciatic nerve, were clearly detectable as separate fascicles, even at the most proximal sites. This was best seen on transversal images.

In the majority of animals, the nerve could be followed in distoproximal direction from where it perforates the gastrocnemius muscle to at about 0–1 cm distal to the trochanter major. Near the trochanter major and at about 5–6 cm distal to this joint, visualisation was often decreased. Retrospective analysis of the images showed that this was caused by the oblique course of the nerve with regard to the ultrasound beam, which reduces the amount of ultrasonic energy reflected back to the probe. Consequently, the echogenicity of the nerve borders is reduced, hampering differentiation of the nerve from the surrounding muscles. More particularly, this appeared to happen when the angle between the ultrasound beam and the nerve was less than 70–75°. In future studies, this problem can therefore easily be avoided by rotating the probe,

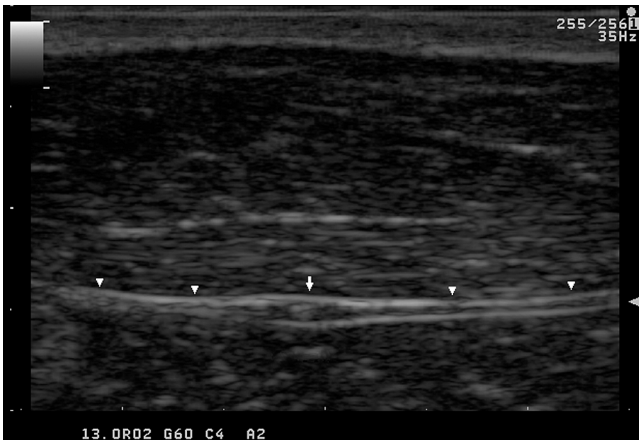

Figure 4. Enlargement of inner nerve diameter at the lesion site (neuroma formation).

Figure 5. Thickening of the nerve with no evident neuroma formation.

so that the ultrasound beam gets more perpendicular to the nerve.

Ultrasound vs. anatomy

Ultrasound images were in good agreement with anatomy. The course of the nerve and its relation to the tibial nerve and surrounding structures matched perfectly with that seen upon anatomical exploration and as described in literature *(Barone et al., 1973; Schmitz and Beer, 2001)*. Also, when the course of the nerve was abnormal, this was clearly seen on ultrasound in agreement with Peer *et al. (2003)* who detected twisting of fascicles around each other in a surgically reconstructed median nerve. Diameters from ultrasound were significantly related to anatomical diameters. However, the scatter in this relation limits strong predictions of anatomical nerve dimensions from transversal ultrasound. Several factors play a role in this scatter. First, from ultrasound, we measured the diameter of the hypoechoic inside of the nerve because the outer border is usually less well defined in transversal images *(Nakamichi and Tachibana, 2002)*, while anatomically, only the outer nerve diameter could be measured. Besides resulting in a negative offset of the ultrasound diameter with regard to the anatomical diameter, this also adds variability in the relation because of variations in thickness of the nerve border and in the amount of extraneural scarring. Second, *in vivo* anatomical measurements, although performed underneath a microscope, will also have measurement errors because of errors in positioning of the calliper gauge and because surgical exposure was needed. The latter could have resulted in altered nerve dimensions because of changes in the mechanical forces of the surrounding structures acting upon the nerve whereas ultrasound measures *in vivo* dimensions in the undisturbed situation.

Because the proximal part of the peroneal nerve was confused with the tibial nerve in one case, on longitudinal scanning, it is advisable to always perform recordings in both longitudinal and transversal directions.

Nerve thickening

Ultrasound was able to show local nerve thickening at the lesion site. More interestingly, it seems to be able to differentiate between neuroma formation (intraneural swelling) and external diameter enlargement (epineural swelling). This potentially is of great value in the clinical situation where visual nerve inspection cannot differentiate between internal and external enlargement of nerve diameter, and both causes require a different treatment regimen. Nerve compression because of a swollen epineurium often requires another treatment than neuroma formation. Further study is required to determine the predictive value of ultrasound in differentiating between these situations through comparison with nerve histology.

With ultrasound, nerve enlargement was measured from longitudinal images. Consequently, the nerve diameter was measured in the sagittal body plane. Anatomically though, diameters could only reliably be measured in the medial–lateral direction (coronal body plane) because diameters were measured underneath a dissection microscope. This microscope could not be used to measure dimensions in the direction perpendicular to the viewing plane. We therefore could have missed nerve thickenings that extend

Table 2. Predictive values for nerve enlargement from ultrasound with regard to *in vivo* anatomy after applying a cut-off of a 0.5-mm increase in nerve diameter for both ultrasound and anatomy.

	Ultrasound inner diameter anatomy diameter − fat	Ultrasound outer diameter anatomy diameter + fat
Positive predictive value	0.83	0.85
Negative predictive value	0.17	0.50
Number of nerves (*n*)	18	19

Values are shown for ultrasound inner nerve diameter against anatomical diameter excluding fat (left column) and for ultrasound outer diameter against anatomical diameter including fat (right column).

predominantly in the medial–lateral direction. This might explain the relatively poor PPV and NPV, although this could also partly be explained by the factors mentioned above. The predictive value of ultrasound regarding diameters including fat is of limited value, although it might be of use in the evaluation of fat grafts, which are commonly used for compression and traction neuropathies *(Botte et al., 1996)*.

Further applications

An interesting application of nerve ultrasound would be the non-invasive evaluation of the progress of nerve regeneration. Peripheral nerves undergo structural changes after trauma; because axons distal to the lesion degenerate, their endoneurial tubes collapse. Upon regeneration, proximal axons send off sprouts, which invade the distal segment. These structural changes might alter the overall echogenicity of the nerve interior during the course of degeneration and regeneration. If it were possible to measure these changes, this would have large value for both neuroscience and clinical management of nerve lesions, because the progress of regeneration can presently only be measured reliably in an invasive way before the target organs are reinnervated, a process that can take many months. To assess the potential of ultrasound for this application, we retrospectively measured the echogenicity (mean value of grayscale histogram) of a 5-mm-long segment of the nerve interior at about 3 cm distal to the lesion ($n = 11$). We compared these values with electrically evoked compound nerve action potentials (CNAPs) from these nerves (which were recorded for different purposes). Because the size of these potentials is roughly proportional to the number of excitable nerve fibres present, the CNAP can be seen as a measure of the extent of regeneration. Unfortunately, we found no useful correlation between these measurements (Spearman $\rho = 0.31$, $p = 0.36$). It therefore seems that the dimensions of the structural changes are too small to change the echogenicity of the nerve interior upon regeneration.

Because local nerve thickenings could be detected in our study, ultrasound could also be of use in experimental studies on nerve-thickening neuropathies and nerve sheet tumours. The ultrasonic appearance of the latter is very similar to the neuromas encountered in this study *(Lin and Martel, 2001)*.

Other possible applications include ultrasound-guided injection of topical medications (e.g., neural growth factors) and monitoring the status of neural implants like nerve cuffs, implantable microstimulators *(Peng et al., 2004)* and microelectrode arrays *(Branner et al., 2004)*.

In conclusion, ultrasound imaging of the rabbit peroneal nerve is very feasible. Like in humans, local nerve thickening can be detected. Preliminary data indicate that ultrasound can differentiate between true neuromas on one hand and epineural swelling and external nerve enlargement on the other.

Acknowledgements

The authors are grateful to the Vereniging Trustfonds Erasmus Universiteit for funding lease of the ultrasound equipment, Dirk Duncker, Monique de Waard, Elza van Deel, and Rob van Bremen for their helpfulness and lending their equipment and Wim Hop for statistical advice.

References

Barone R, Pavaux C, Blin PC, Cuq P (1973). Atlas D'anatomie Du Lapin (Atlas of Rabbit Anatomy). Masson, Paris.

Beekman R, Visser LH (2002). Sonographic detection of diffuse peripheral nerve enlargement in hereditary neuropathy with liability to pressure palsies. J Clin Ultrasound 30:433–436.

Beekman R, Visser LH (2003). Sonography in the diagnosis of carpal tunnel syndrome: a critical review of the literature. Muscle Nerve 27:26–33.

Botte MJ, von Schroeder HP, Abrams RA, Gellman H (1996). Recurrent carpal tunnel syndrome. Hand Clin 12:731–743.

Branner A, Stein RB, Fernandez E, Aoyagi Y, Normann RA (2004). Long-term stimulation and recording with a penetrating microelectrode array in cat sciatic nerve. IEEE Trans Biomed Eng 51:146–157.

Lee D, van Holsbeeck MT, Janevski PK, Ganos DL, Ditmars DM, Darian VB (1999). Diagnosis of carpal tunnel syndrome. Ultrasound versus electromyography. Radiol Clin North Am 37:859–872, x.

Lin J, Martel W (2001). Cross-sectional imaging of peripheral nerve sheath tumors: characteristic signs on CT, MR imaging, and sonography. AJR Am J Roentgenol 176:75–82.

Nakamichi K, Tachibana S (2002). Ultrasonographic measurement of median nerve cross-sectional area in idiopathic carpal tunnel syndrome: diagnostic accuracy. Muscle Nerve 26:798–803.

Peer S, Harpf C, Willeit J, Piza-Katzer H, Bodner G (2003). Sonographic evaluation of primary peripheral nerve repair. J Ultrasound Med 22:1317–1322.

Peng CW, Chen JJ, Lin CC, Poon PW, Liang CK, Lin KP (2004). High frequency block of selected axons using an implantable microstimulator. J Neurosci Methods 134:81–90.

Quinn TJ, Jacobson JA, Craig JG, van Holsbeeck MT (2000). Sonography of Morton's neuromas. AJR Am J Roentgenol 174:1723–1728.

Schmitz HC, Beer GM (2001). Muscle-sparing approach to the peroneal nerve of the rabbit. Lab Anim 35:334–339.

Silvestri E, Martinoli C, Derchi LE, Bertolotto M, Chiaramondia M, Rosenberg I (1995). Echotexture of peripheral nerves: correlation between US and histologic findings and criteria to differentiate tendons. Radiology 197:291–296.

Stuart RM, Koh ES, Breidahl WH (2004). Sonography of peripheral nerve pathology. AJR Am J Roentgenol 182: 123–129.